GEOLOGIC NOTE

Pore-throat sizes in sandstones, tight sandstones, and shales

Philip H. Nelson

ABSTRACT

Pore-throat sizes in siliciclastic rocks form a continuum from the submillimeter to the nanometer scale. That continuum is documented in this article using previously published data on the pore and pore-throat sizes of conventional reservoir rocks, tight-gas sandstones, and shales. For measures of central tendency (mean, mode, median), pore-throat sizes (diameters) are generally greater than 2 μm in conventional reservoir rocks, range from about 2 to 0.03 μm in tight-gas sandstones, and range from 0.1 to 0.005 μm in shales. Hydrocarbon molecules, asphaltenes, ring structures, paraffins, and methane, form another continuum, ranging from 100 Å (0.01 μm) for asphaltenes to 3.8 Å (0.00038 μm) for methane. The pore-throat size continuum provides a useful perspective for considering (1) the emplacement of petroleum in consolidated siliciclastics and (2) fluid flow through fine-grained source rocks now being exploited as reservoirs.

INTRODUCTION

In the evaluation of conventional oil and gas reservoirs, the distinction between reservoir and seal is clear. For purposes of this article, a conventional reservoir is one in which evidence that buoyant force has formed and maintained the disposition of oil and gas is present. Pore size and pore throats in reservoir rock are large enough to store and deliver economic quantities of petroleum, whereas pore throats in seals are small enough to block the passage of petroleum at the applied level of buoyant pressure. With continued growth in the exploration

Manuscript received June 2, 2008; provisional acceptance July 31, 2008; revised manuscript received October 1, 2008; final acceptance October 24, 2008.
DOI:10.1306/10240808059

AUTHOR

PHILIP H. NELSON ~ *U.S. Geological Survey, Box 25046, Federal Center, Denver, Colorado 80225-0046; pnelson@usgs.gov*

Phil Nelson is a member of the Central Energy Resources Team of the U.S. Geological Survey, which provides assessments of undiscovered oil and gas. He held research positions in mineral exploration with Kennecott Exploration Services, radioactive waste storage with Lawrence Berkeley Laboratory, and petroleum production with Sohio Petroleum Company. His current interests are in the characteristics of tight-gas resources and the pressure and temperature regimes of sedimentary basins.

ACKNOWLEDGEMENTS

Encouragement and comments for expansion and elaboration of the pore-throat spectrum came from several people, including G. Beck of EOG Resources; R. Merkel of Newfield Exploration Company; D. Houseknecht, M. Lewan, N. Fishman, and P. Hackley of the U.S. Geological Survey; and AAPG reviewers T. Olson, V. Hitchings, and R. Worden.

and development of tight-gas sandstones and shale gas, petroleum geoscientists and engineers are increasingly concerned with fluid storage and flow in low-permeability (submillidarcy) systems. In these systems, evidence for buoyancy as a dominant force in the disposition of oil and gas is lacking. Associations among capillary pressure, petrographic description, permeability, and porosity have been documented for a range of reservoir rocks. High-quality reservoir rocks generally have pore sizes greater than 30 μm (macropores) and pore-throat sizes greater than 10 μm. The term ''microporosity'' is applied to pore sizes less than 10 μm, and ''micropore throats'' is the term applied to pore-throat sizes less than 1 μm; such rocks have low permeabilities and high water saturations if water wet. Between the micro and macro limits is a mesoporosity regime (Pittman, 1979; Coalson et al., 1985). Although not used in this article, this terminology recognizes the pore and pore-throat size spectrum, and the examples compiled in this article are compatible with these general definitions. In particular, the 1-μm specification for pore-throat size seems to mark the transition from low-quality conventional reservoir rocks to the regime of tight-gas sandstones. With such small pore throats, high differential gas pressures are required to overcome capillary resistance.

In view of the growing production from rocks with small pore sizes, closely analyzing the properties of rocks that were once considered nonreservoir becomes increasingly important for geologists and petrophysicists, as recovery of gas and oil from fine-grained sandstones, siltstones, and shales blurs the distinction between reservoir and seal. The primary purpose of this article is to document the continuum of pore openings and throat sizes from large to small. To do so, I draw on previously reported measurements of siliciclastic rocks to construct a size spectrum ranging over seven orders of magnitude, a range that accommodates grain sizes at the high end and molecular sizes at the low end. Between these extremes, the spectrum illustrates the downward progression in pore-throat size from conventional reservoir rocks to tight-gas sandstones to shales. Within a given geologic setting, the position of a particular rock unit within the pore-throat spectrum determines the likelihood that it will contain a petroleum resource. In fact, a pore-throat cutoff is sometimes used to compute net pay (e.g., Kolodzie, 1980) and appears to offer advantages over a porosity or permeability cutoff in low-permeability rocks. Beyond establishment of cutoffs for economic recovery with a given technology, questions arise regarding the fundamental limitations governing emplacement and extractability of hydrocarbons from low-porosity, low-permeability rocks. This article does not attempt to answer these difficult questions but does provide a conceptual framework for addressing them.

Petroleum geologists are accustomed to characterizing reservoir rocks in terms of porosity and permeability instead of pore-throat size. Each decade (order of magnitude, or factor of 10) of change in pore-throat size corresponds approximately to two decades of permeability change; for example, a 5% porosity rock with an entry pore-throat size of 1 μm can have a permeability of 11.2 μd, but if the pore-throat size is 0.1 μm, the permeability is 0.112 μd. A size scale is better suited for consideration of gas charging than a permeability scale because capillary pressure corresponds inversely to pore-throat size; in fact, capillary pressure measurements are used to determine the pore-throat size. In this article, the term ''size'' equates either with diameter, if a pore throat is considered as cylindrical, or with width, if a pore throat is characterized as a thin slot.

PORE THROATS AND PORES

Wardlaw and Cassan (1979) measured the grain-particle size, pore size, and pore-throat size for 27 sandstone samples from various locations worldwide and of various geologic ages. Core depths range from 1000 to 3000 m (3280 to 9840 ft). This sample set was chosen to represent sandstones with permeability values greater than 1 md. The mean particle size, as determined from thin sections, ranges from coarse silt to medium grain size. The mean pore size was determined by measuring the diameter of the largest inscribed circle fit within pores in resin casts of the rock samples. The

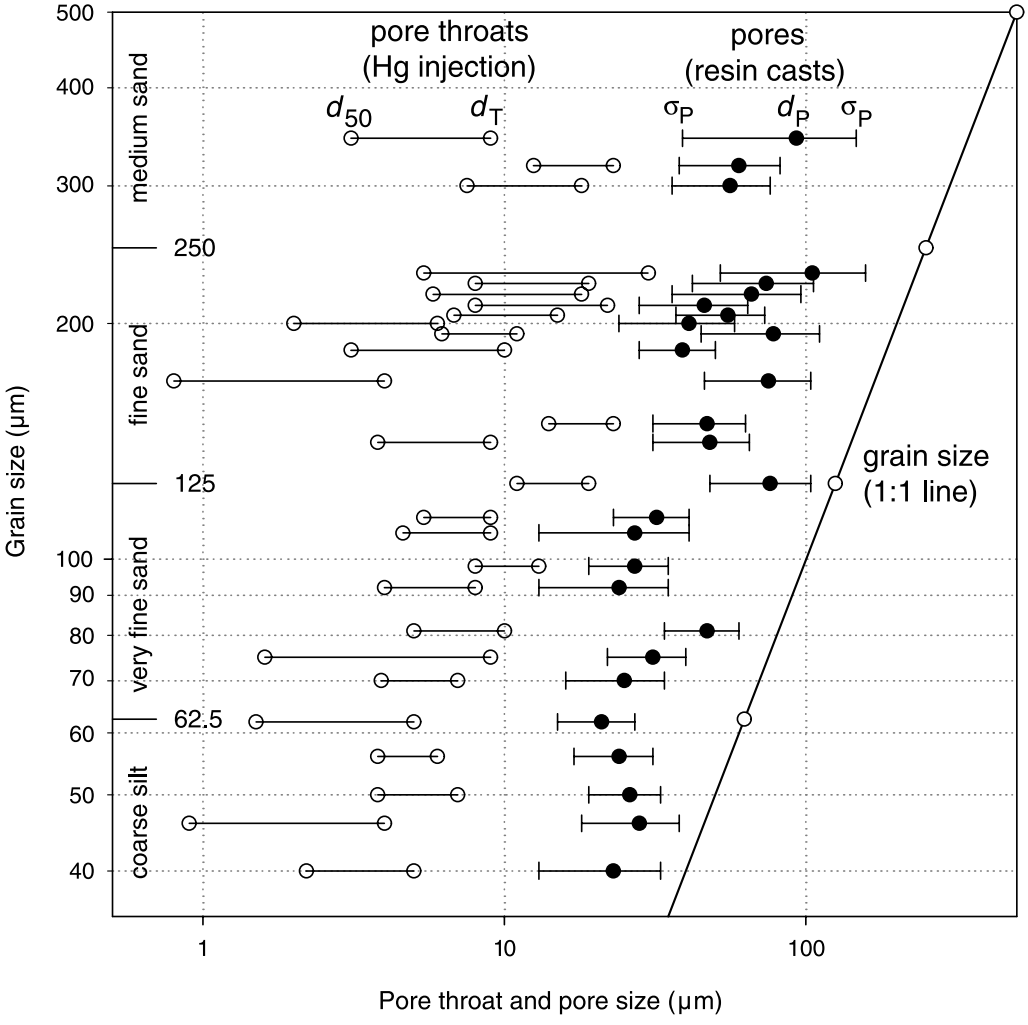

Figure 1. Grain size, pore size, and pore-throat size for 27 sandstone samples (Wardlaw and Cassan, 1979). The mean particle size serves as the ordinate, with other sizes plotted on the abscissa. Mean pore size d_P and standard deviation σ_p were determined from resin casts of pore space. The pore-throat size at threshold entry pressure, d_T, and at 50% mercury saturation, d_{50}, was determined by mercury injection.

pore-throat size was determined by mercury injection at threshold entry pressure and at 50% mercury saturation. These parameters are shown in Figure 1.

For the samples studied by Wardlaw and Cassan, the mean grain size is consistently greater than the mean pore size plus one standard deviation, and the mean pore size minus one standard deviation is consistently greater than the largest pore-throat size determined by mercury injection (Figure 1). This ordering holds for grain sizes ranging from coarse silt to medium sand. Only the largest part of the pore-throat-size spectrum is shown, the smallest pore throats are not represented. Pores and pore throats generally (but erratically) decrease as grain size decreases. Differences in sorting among samples may account for the observation that the pores and pore throats of coarse silt and very fine sand samples are larger with respect to grain size than those of the fine and medium sands. At the smaller grain sizes, the pore-throat size at threshold entry pressure, d_T, is about 1/10 of the mean grain size.

THE PORE-THROAT-SIZE SPECTRUM

Figure 2 shows pore-throat sizes of sandstones, tight-gas sandstones, and shales, and the size of selected molecules. The horizontal axis of the graph extends over seven orders of magnitude, from 10^{-4} μm (1 Å) to 10^3 μm (1 mm). (Orders of magnitude are deceptive; a length of 1 Å has the same relation to 1 mm as does a 1-mm length to 10 km [6 mi].) The sedimentological scale for grain size, which divides the spatial scale from 1 mm to 0.49 μm into factors of two, is shown in the lower right of the graph, along with a scale for Tyler screen sizes used for sieving unconsolidated materials. The resolution of methods for examining pore space

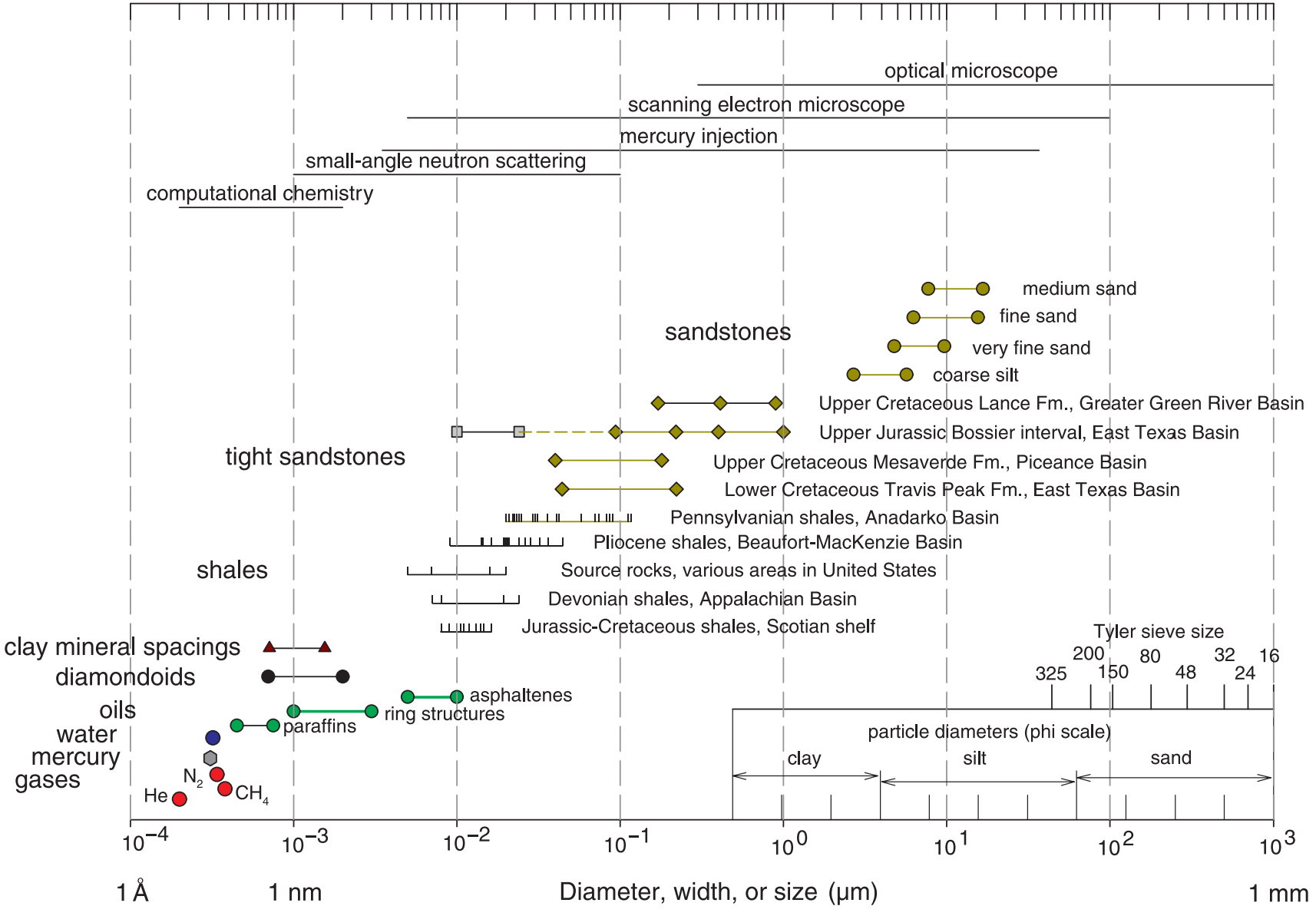

Figure 2. Sizes of molecules and pore throats in siliciclastic rocks on a logarithmic scale covering seven orders of magnitude. Measurement methods are shown at the top of the graph, and scales used for solid particles are shown at the lower right. The symbols show pore-throat sizes for four sandstones, four tight sandstones, and five shales. Ranges of clay mineral spacings, diamondoids, and three oils, and molecular diameters of water, mercury, and three gases are also shown. The sources of data and measurement methods for each sample set are discussed in the text.

on the microscopic scale is shown at the top of the graph. In particular, the lower limit of 0.0035 μm for mercury injection corresponds to a mercury injection pressure of 60,000 psi. Pore-throat sizes for clastic rocks in various formations are shown in the center of the graph; in the following sections, sizes are discussed in micrometers for sandstones, tight sandstones, and shales, and in angstroms and nanometers for molecules.

Characterization of the pore-throat size of a rock sample requires the choice of (1) a method of measurement, (2) a model for converting the measurement to a dimension, and (3) selection of a parameter to represent the resulting size distribution. Usually, mercury injection is used as the measurement method, although gas-flow methods were used for two of the examples described in this article. The model used for conversion of mercury pressure to pore-throat size, known as the Washburn equation, assumes that mercury invades a series of cylindrical (capillary) openings. Other models assume that the openings are composed of parallel plates (slots), and more elaborate models break the pore space into two shapes, one controlling flow and the other providing storage. Finally, to represent the distribution of pore-throat size, authors may choose a measure of central tendency (mean, mode, or median) or a dimension associated with a specified saturation of the invading fluid (10 or 35% mercury saturation) or an inflection point on a graph of pressure vs. volume of invading fluid. Because different authors choose different methods, models, and representative parameters, the following descriptions provide background information for each sample set shown in Figure 2. In addition, Table 1 provides an abbreviated overview of the data sets shown in Figure 2; values in Table 1 give statistics for one point on the pore-throat distribution curve, whereas some cases shown in Figure 2 provide more information regarding the distribution, as described next.

Sandstones

Arithmetic averages of pore-throat data (Figure 1) from Wardlaw and Cassan (1979) are plotted in Figure 2. The left circle is the average for pore-throat size at 50% mercury saturation and the right circle is the average of the entry threshold sizes. Statistics for entry threshold sizes are given in the first four rows of Table 1. These data represent rocks of fair to good reservoir quality (average porosity of 21% and geometric mean permeability of 30 md for 27 samples) and serve as a reference for rocks with pore dimensions of smaller size.

Upper Cretaceous Lance Formation, Greater Green River Basin, Wyoming

Gas is produced from low-permeability sandstones of the Upper Cretaceous Lance Formation at Jonah field in the Greater Green River Basin, Wyoming, at depths of 8000–12,000 ft (2438–3657 m) (Dubois et al., 2004). Grain size ranges from coarse silt to fine-grained sandstone. Based on core tests and mercury injection results for seven samples from the middle and upper Lance made available by the Encana Corporation, permeability ranges from 3 to 338 μd, porosity ranges from 4.6 to 10.4%, and pore-throat size is 0.89 μm at threshold entry pressure, 0.41 μm at 35% mercury saturation, and 0.17 μm at 50% mercury saturation (Figure 2).

Upper Jurassic Bossier Interval, East Texas

The Upper Jurassic Bossier Formation sandstones produce gas from depths of 12,000–18,000 ft (3657–5486 m) in the East Texas Basin. Rushing et al. (2004, p. 379) described the Bossier interval as ''a thick, lithologically complex black to gray-black shale interbedded with fine-grained argillaceous sandstone.'' Thirteen samples of sandstones from the Bossier interval were classed into four rock types of reservoir quality, with characteristic (modal) pore-throat diameters of 0.094, 0.220, 0.40, and 1.0 μm, designated by four diamonds in Figure 2, and two nonreservoir rock types, 0.010 and 0.024 μm, designated by two squares (Rushing et al., 2004). The pore-throat size was determined by mercury injection. Permeability and porosity values were determined for a larger sample set. Permeability and porosity ranges are 0.3–500 μd

Table 1. Summary of Measurements of Pore-Throat Size and Other Parameters for Siliciclastic Rocks, Selected from Published Sources*

Source of Samples	No.**	Pore-Throat Diameter (μm)			Method**	Model**	Statistic**	Porosity (%)	Permeability	Depth (ft)
		Min.	Max.	Avg.						
Medium-grained sandstones, various, worldwide	3	9.000	23.000	16.667	Hg	C	ET	14	25.5 md	6560
Fine-grained sandstones, various, worldwide	12	4.000	30.000	15.500	Hg	C	ET	18.1	19.6 md	6560
Very fine-grained sandstones, various worldwide	6	8.000	13.000	9.667	Hg	C	ET	24.2	109.7 md	6560
Coarse siltstones, various, worldwide	6	4.000	7.000	5.667	Hg	C	ET	26.3	22.3 md	6560
Upper Cretaceous Lance Formation, Greater Green River Basin	7	0.362	2.520	0.895	Hg	C	ET	7.5	17.7 μd	8713
Upper Jurassic Bossier interval, East Texas Basin, reservoir rock	9	0.094	1.000	–	Hg	C	MO	7.5	12.2 μd	12,000
Upper Jurassic Bossier interval, East Texas Basin, nonreservoir rock	4	0.010	0.024	–	Hg	C	MO	4.5	0.25 μd	12,000
Upper Cretaceous Mesaverde Formation, Piceance Basin	44	0.040	0.180	–	gas	T	CO	7	2.1 μd	6513
Lower Cretaceous Travis Peak Formation, East Texas Basin	13	0.044	0.220	0.118	gas	T	CO	4.9	1.5 μd	9347
Pennsylvanian shales, Anadarko Basin	21	0.020	0.116	0.050	Hg	C	ET	–	–	12,354
Pliocene shales, Beaufort-Mackenzie Basin	20	0.009	0.044	0.023	Hg	C	GM	7.5	–	8885
Source rocks, various, United States	5	0.005	0.020	0.012	V	S	ME	–	–	–
Devonian shales, Appalachian Basin, organic poor	6	0.007	0.008	0.008	Hg	C	ME	7.2	1.4 μd	Outcrop
Devonian shales, Appalachian Basin, organic rich	6	0.019	0.024	0.022	Hg	C	ME	3.6	5.1 nd	Outcrop
Jurassic and Cretaceous shales, Scotian shelf	10	0.009	0.016	0.012	Hg	C	GM	4.9	1.9 nd	16,800

*The pore-throat-size ranges and averages given here do not match values shown in Figure 2 in all cases. Porosity value is the arithmetic average; permeability value is the geometric mean; depth value is the average depth. Further details and references are given in the text.

**No. = number of samples. Method: Hg = mercury injection; gas = gas flow; V = both mercury injection and small angle neutron scattering. Model: C = cylindrical capillary; T = tabular; S = spherical in the case of small angle neutron scattering. Statistic: ET = entry threshold; MO = mode; CO = computational; GM = geometric mean; ME = median.

and 1–14% for the four rock types of reservoir quality, and 0.03–20 μd and 1–8% for the two rock types of nonreservoir quality.

Upper Cretaceous Mesaverde Formation, Piceance Basin, Colorado

Soeder and Randolph (1987) documented the existence of narrow slot pores in tight-gas sandstones of the Upper Cretaceous Mesaverde Formation. Located between grains with extensive quartz overgrowths, the slot pores were identified at the magnification limit of an optical microscope then examined more closely with a scanning electron microscope. The porosity of 44 samples ranges from 3 to 11%, and permeability ranges from 0.5 to 9 μd. After drying in a relative-humidity oven, the permeability to gas was determined in a steady-state apparatus at net confining pressure, and the slot width was computed using a method described by Randolph et al. (1984). All core samples had characteristic widths between 0.04 and 0.18 μm, establishing the range shown in Figure 2.

Lower Cretaceous Travis Peak Formation, East Texas

In a follow-up study with the same equipment used by Soeder and Randolph (1987), Soeder and Chowdiah (1990) measured the storage and flow properties of 13 deltaic sandstone samples from the Lower Cretaceous Travis Peak Formation in a well in east Texas, at depths of 8250–9932 ft (2514–3027 m). Porosities range from 3.0 to 6.3%, permeabilities range from 0.09 to 16.5 μd, and pore widths determined from gas flow (hereafter referred to as w-gas) range from 0.044 to 0.22 μm (Figure 2). Pore widths also were determined by mercury injection (w-Hg) for the same 13 samples. The w-Hg distribution was broader than the w-gas distribution, although w-Hg was substantially greater (typically 30% greater) than w-gas for 10 of the 13 samples, and the median of w-Hg was 1.15 greater than w-gas. Disparities of this magnitude are not surprising for two different invading fluids and computational models. Only the distribution for w-gas is shown in Figure 2.

Pennsylvanian Shales, Anadarko Basin, Oklahoma

Mercury injection measurements on 21 shales and sandy shales from wells distributed across the Anadarko Basin, with depths ranging from 5760 to 18,950 ft (1756 to 5776 m), were tabulated by Cranganu and Villa (2006). The pore-throat size was determined using the injection pressure obtained from extrapolation of the plateau of the mercury injection curve to zero mercury saturation, hence these values are threshold or initial-connectivity values. The minimum, arithmetic mean, and maximum pore-throat diameters of the 21 samples (individual values are shown in Figure 2) are 0.020, 0.050, and 0.116 μm, respectively. Values of porosity and permeability were not cited for these samples.

Pliocene Shales, Beaufort-Mackenzie Basin, Canada

Pore-throat distributions for shale samples from wells in the subsiding late Tertiary Beaufort-Mackenzie Basin were determined by mercury injection by Katsube and Issler (1993). They observed that both the porosity and geometric-mean pore-throat size of the shales decrease steadily from 1 km (0.6 mi) to around 2 km (1.2 mi) in depth and remain constant below 2 km (1.2 mi). For 20 samples obtained from depths greater than 2 km (1.2 mi), porosities range from 5.1 to 12.6%, and the geometric-mean pore-throat sizes range from 0.009 to 0.044 μm, with nine values clustered around 0.020 μm. Permeability was not measured.

Source Rocks, United States

Citing two sources, Hunt (1996, his table 8-2) tabulated median pore diameters and porosities for five shale source rocks in the United States: Bakken: 0.005 μm, 4.3%; Cherokee: 0.007 μm, 5.2%; Monterey: 0.010 μm, 8.5%; Monterey: 0.016 μm, 12.7%; and Tertiary Gulf Coast: 0.020 μm, 15%. The pore diameters were determined by either mercury injection or small-angle neutron scattering. Median pore diameters for these five samples are plotted

in Figure 2. Two of the formations (Bakken and Monterey) also contain reservoirs that produce hydrocarbons.

Devonian Shales, Appalachian Basin

Properties of four Devonian shales from the Appalachian Basin in western New York were determined by Lash (2006) and Lash and Blood (2006). The pore diameters, porosities, and permeabilities of two organic-rich shales, with total organic carbon (TOC) content greater than 2.3%, were Dunkirk, 0.007 μm, 3.2%, 0.0026 μd; and Rhinestreet, 0.008 μm, 3.9%, 0.01 μd. For two organic-poor shales, with TOC less than 0.9%, the values of pore diameter, porosity, and permeability are Hanover, 0.024 μm, 6.0%, 2.0 μd; and Cashaqua 0.019 μm, 8.5%, 1.0 μd. The values represent either median or average values of pore diameter, determined by mercury injection on three samples of each shale. Permeabilities of the organic-poor shales are roughly 100 times greater than the organic-rich shales. Low permeabilities and small pore throats of the organic-rich shales were attributed to a strongly oriented microfabric, lack of bioturbation, and squeezing of ductile organic matter into void spaces.

Jurassic and Cretaceous Shales, Scotian Shelf, Canada

Ten samples from three wells at depths between 15,300 and 18,300 ft (4663 and 5578 m) were analyzed with mercury injection (Katsube et al., 1991). Porosities range from 1.5 to 8.4%. Permeability measured with a pulse-decay method on two samples yielded values of 0.8 and 4.2 nd at in-situ effective stress. The geometric means of the pore-throat-size distributions, ranging from 0.008 to 0.016 μm, are shown in Figure 2. Half the samples have scarcely any pore-throat sizes greater than 0.1 μm, and the other half have only a small fraction of pore sizes greater than 1.0 μm. Three of the 10 samples were also used in compaction tests in which permeability and resistivity were measured. Pore-throat sizes computed from these measurements are comparable to, or somewhat greater than, the pore-throat sizes determined by mercury injection (Bowers and Katsube, 2002).

CLAY-MINERAL SPACINGS, NANOSTRUCTURES, AND MOLECULAR SIZES

At some scale in a porous media, solid-fluid interactions disrupt fluid-fluid interactions. At this scale, discussed here using nanometers and angstroms as units, a fluid cannot be represented in terms of its macroscopic properties (such as viscosity), and Darcy's law is invalid. This transition from satisfactory to inadequate characterization of flow with macroscopic parameters appears to occur where pore sizes are on the order of 10 nm or less; for example, laboratory study of smectite-water systems indicates that the thickness of the perturbed water film extends at least 3.5 nm away from the clay surface, and at the very least, the structure of water differs from that of normal water for three molecular layers (~1.0 nm) adjacent to a silicate surface (Mitchell and Soga, 2005). Computational models incorporating molecular positions and interactions can be used to understand fluid flow in openings with sizes less than 10 nm (Cushman, 1997). A non-Darcy flow regime probably exists in some part of the pore network in shales and particularly in source rocks. Thus, the following size values for minerals and fluids, chosen to compliment the pore-throat-size spectrum, cannot be readily construed in terms of the concepts of capillarity and flow that are useful at larger scales.

The basal spacing in clay minerals is the distance between repeated structures, or the size of the unit cell, and is a reasonable mineralogical parameter for this compilation. The basal spacing for kaolinite, illite, and chlorite is 7.1, 10.0, and 14.3 Å, respectively. The basal spacing for collapsed montmorillonite is 9.6 Å, and the spacing for a common form with two layers of hydration is 15.5 Å (Deer et al., 1966). A range of 7.1–15.5 Å (0.71–1.55 nm) is illustrated in Figure 2. These values indicate the spacings between hydrated layers or exchangeable cations.

Hydrocarbons having a cagelike crystalline structure called diamondoids have been separated from petroleum (Dahl et al., 2003). The dimensions of lower diamondoids, which have one to three cage-shaped units, are less than 1 nm; higher

diamondoids with more than four cage-shaped units have dimensions of 1–2 nm (Dahl et al., 2003). Nanominerals, particularly oxides and sulfides of iron and zinc, have been identified in the laboratory and in natural settings, have dimensions ranging upward from 0.7 nm, and are the subject of current study (Hochella et al., 2008).

Approximate, effective diameters of gas and liquid molecules of interest to petroleum geoscientists are also shown in Figure 2 (Tissot and Welte, 1978; Hunt, 1996). The diameter for helium (commonly used to measure porosity) cited by Tissot and Welte is 2.0 Å or 0.2 nm. By way of comparison, the van der Waals diameter for helium is 2.8 Å or 0.28 nm (Bondi, 1964). The van der Waals diameter is related to the volume that must be accounted for in correcting the perfect gas law for finite atomic size. The effective molecular diameters for nitrogen gas molecules N_2 are 3.4 Å; methane CH_4, 3.8 Å; water, 3.2 Å; complex ring structures, 10–30 Å; and asphaltene molecules, 50–100 Å (Tissot and Welte, 1978, their table III.2.1). For paraffins, combined width-height values range from 4.5 Å for normal paraffins to 7.5 Å for branched-chain paraffins (Jimenez-Cruz and Laredo, 2004). The diameter of mercury as determined by two methods is 3.1 and 3.3 Å (Bondi, 1964); the value of 3.1 Å (0.31 nm) is plotted in Figure 2.

PERMEABILITY AS A MEASURE OF PORE-THROAT SIZE

How does the pore-size scale of Figure 2 relate to permeability? Permeability has the dimensions of length squared, and various authors have shown that permeability is proportional to the square of pore-throat size times a porosity factor (Nelson and Batzle, 2006). A relation derived by Katz and Thompson (1986) can be written as

$$k \approx 4.48\, d^2\, \varphi^2 \qquad (1)$$

where k is the permeability in millidarcies, d is the pore size in micrometers corresponding to the pressure at which mercury first forms a continuous connected pathway through the sample as measured by the inflection point on a capillary pressure curve, and φ is the fractional porosity. As an example, data from multiple samples of a tight-gas sandstone span more than six decades of permeability and range from 2 to 18% in porosity (Figure 3A). These data are transformed in accordance with equation 1 and displayed as pore size (diameter) and porosity in Figure 3B. The scales in Figure 3 are constructed so that one decade of pore- size change corresponds to two decades of permeability change. If permeability was proportional only to the square of pore-throat size, then the two data clouds in Figure 3A and B would have the same horizontal extent. Because porosity is higher where permeability is higher and lower where permeability is lower, the porosity term in equation 1 causes the pore-throat-size distribution computed from equation 1 in Figure 3B to be less broad than the permeability distribution of Figure 3A. Consider the four samples represented with open circles. The sample with a permeability of 10 μd and porosity of 4.8% in Figure 3A transforms to a pore size of 1 μm in Figure 3B, the (1.1 md, 9.2%) sample transforms to a pore size of 5.4 μm, and the two samples on the ends of the permeability distribution migrate inward. This exercise demonstrates that permeability serves as an imperfect length scale because of the nonunique relation between pore-throat size and flow rate, and that an equivalence between permeability and pore-throat size depends on the algorithm used to relate them and the porosity of the sample.

The pore-throat size d chosen by Katz and Thompson (1986) in equation 1 corresponds to the high end of the pore-throat-size distribution and correspondingly to a low value of mercury injection pressure and mercury saturation. Other relations between permeability and pore-throat size differ from equation 1 because a different point on the pore-throat-size distribution (such as 35% mercury saturation) is chosen to represent the pore-throat size (Figure 3C). Consequently, the cloud of points in Figure 3A migrates to smaller pore throats in Figure 3C because higher values of mercury saturation (higher injection pressure) are used to characterize the pore-throat size. The selection of a permeability-to-pore-throat transform poses the same question as the representation of mercury injection

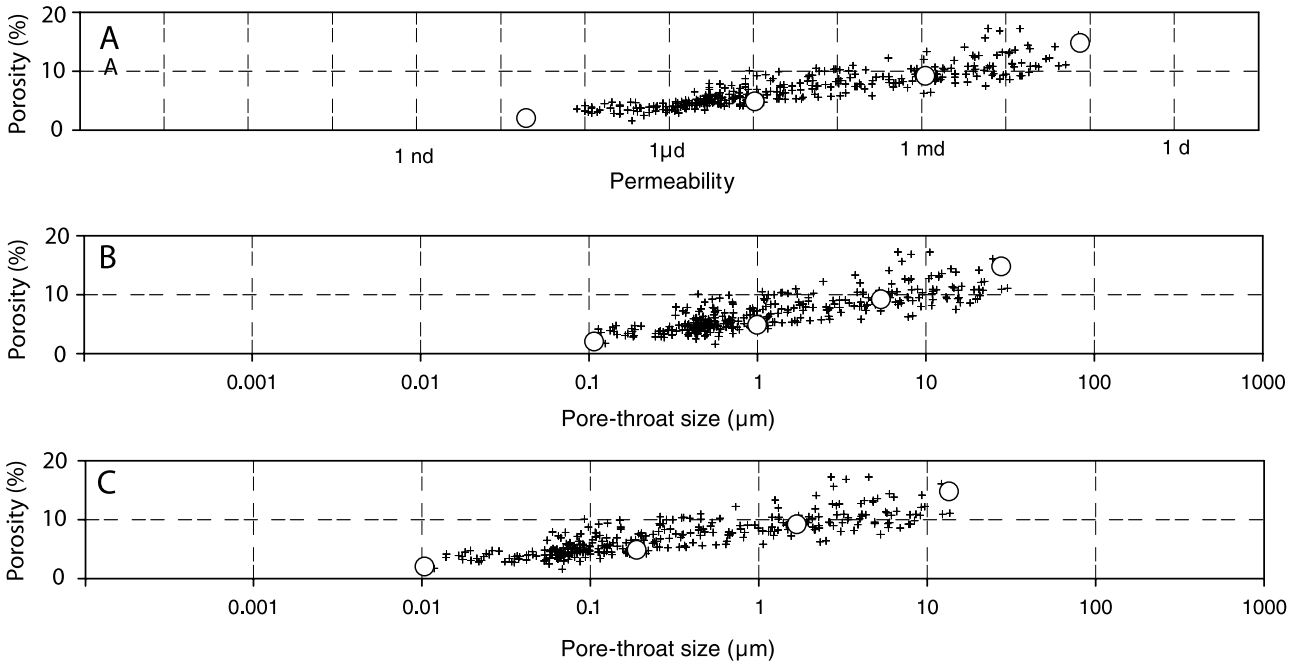

Figure 3. (A) Permeability and porosity data from channel sandstones of the Travis Peak Formation in east Texas from Luffel et al. (1991). The vertical axis is a compressed porosity scale, ranging from 0 to 20%. (B) Pore-throat size computed from the data of panel A using the equation of Katz and Thompson (1986). Four data points are displayed as open circles to illustrate the transform from permeability and porosity to pore-throat size and porosity. (C) Pore-throat size computed from panel A using an algorithm referred to as the Winland equation, in which the pore-throat size corresponds to the pressure attained at 35% mercury saturation.

data with a single pore-throat value (threshold, mode, median, or average), that is, which part of the pore-throat-size spectrum in a sample should be used to represent the sample? The transform selected in Figure 3B corresponds to the pore-throat size determined with the threshold entry pressure, and the transform represented in Figure 3C is closer to the midpoint of the pore-throat-size distribution.

SENSITIVITY TO CONFINING PRESSURE

The importance of slot pores, also called sheet pores, was documented by Morrow (1985), Brower and Morrow (1985), and Kilmer et al. (1987). These studies prepared pore casts showing the existence of sheet pores, demonstrated the sensitivity of permeability and pore width to confining stress, and used gas-flow experiments to derive a mean crack thickness. Slot pores comprise a honeycomblike structure, bounding the flat surfaces of adjacent grains. Their high asperity results in large changes in slot width with changes in confining pressure. For example, a suite of 20 samples with microdarcy permeability, porosities in the 3–7% range, and high carbonate cement had average pore widths of 0.23 and 0.080 µm at confining pressures of 500 and 5000 psi, respectively (Morrow, 1985, his table 17). The geometric mean permeability decreased from 10 to 0.6 µd at these same confining pressures.

Based on studies of tight-gas sandstones from the Frontier, Mesaverde, and Travis Peak formations, Soeder and Chowdiah (1990) concluded that tight-gas sandstones are distinguished petrographically from sandstones of higher permeability by (1) loss of primary porosity through diagenesis, (2) occurrence of most porosity in secondary (dissolved) pore space, and (3) the existence of slot pores between adjoining quartz overgrowths on sand grains that form the interconnected pathways for fluid flow. In summary, secondary-solution pores comprise the storage porosity and the width of slot pores sets the permeability to flow.

A similar result is observed in shales. Bowers and Katsube (2002) used a combination of gas flow

and electrical resistivity measurements at varying confining pressure to distinguish between storage porosity and connecting porosity, the latter comprises sheetlike pores that control flow. From the analysis of experimental data, they showed that storage porosity does not change much with stress, whereas connecting porosity decreases by a factor of 3–10 as effective pressure increases by 7000 psi (48 MPa). At an effective pressure of 5800 psi (40 MPa), they determined connecting pore widths of 2, 4, 4, 6, and 15 nm in five Canadian shales. Changes in effective stress, whether induced by loading or unloading via pore pressure increases, are likely to affect transport properties more than storage properties in both tight-gas sandstones and shales.

SUMMARY

Different researchers report different measures (geometric mean, arithmetic mean, median, and threshold) to represent the pore-throat-size distribution. Although not too apparent on the logarithmic scale of Figure 2, these differences in measure should be kept in mind when making comparisons across orders of magnitude in size. For measures of central tendency (mean, mode, and median), reservoir sandstones generally have pore sizes greater than 20 μm and pore-throat sizes greater than 2 μm (Figure 1). Tight-gas sandstones have pore-throat sizes ranging from about 2 to 0.03 μm (Figure 2, Table 1). Pore-throat sizes in shales range from 0.005 μm, close to the lower limit of resolution for mercury injection, up to 0.05 μm, with some samples as high as 0.1 μm. These size ranges are based on the collection of measurements summarized in this article and stand to be modified as more data become available. Based on this compilation, pore-throat sizes in siliciclastic rocks form a continuum from 20 to 0.005 μm. The smallest detectable (mean) pore-throat sizes in shales are comparable to the size of asphaltene molecules and roughly 10 times greater than the diameters of water and methane.

Permeability is the preferred parameter when considering petroleum production, but pore-throat size is the preferred length scale when considering gas percolation because it determines the differential pressure required to saturate the pore space. Permeability has the dimensions of length squared and, with porosity as an additional factor, can be converted to pore-throat size; however, the choice of transform requires a choice of measure of the pore-throat distribution.

Conventional reservoirs consist of permeable rocks overlain by a seal or low-permeability layer. On the pore-size spectrum, a large gap exists between the seal (~0.05 μm) and what is normally considered to be the reservoir rock (~2.0 μm). This is not the case in low-permeability gas systems where little or no gap between productive and nonproductive rock units in terms of pore-throat size exists. Instead, petroleum-productive rock units and nonproductive units are interlayered spatially and can have overlapping values of pore and pore-throat size. Figure 2 serves as a reference when considering the disposition of fluids in consolidated siliciclastics.

REFERENCES CITED

Bondi, A., 1964, Van der Waals volumes and radii: Journal of Physical Chemistry, v. 68, no. 3, p. 441–451.

Bowers, G. L., and T. J. Katsube, 2002, The role of shale pore structure on the sensitivity of wire-line logs to overpressure, *in* A. Huffman and G. Bowers, eds., Pressure regimes in sedimentary basins and their prediction: AAPG Memoir 76, p. 43–60.

Brower, K. R., and N. R. Morrow, 1985, Fluid flow in cracks as related to low-permeability gas sands: Society of Petroleum Engineers Journal, v. 25, p. 191–201.

Coalson, E. B., D. J. Hartmann, and J. B. Thomas, 1985, Productive characteristics of common reservoir porosity types: Bulletin of the South Texas Geological Society, v. 25, no. 6, p. 35–51.

Cranganu, C., and M. A. Villa, 2006, Capillary sealing as an overpressure mechanism in the Anadarko Basin: AAPG, Search and Discovery Article 40187: www.searchanddiscovery.com (accessed February 25, 2008).

Cushman, J. H., 1997, The physics of fluids in hierarchical porous media: Angstroms to miles: Dordrecht, Netherlands, Kluwer Academic Publishers, 467 p.

Dahl, J. E., S. G. Liu, and R. M. K. Carlson, 2003, Isolation and structure of higher diamondoids, nanometer-sized diamond molecules: Science, v. 299, p. 96–99.

Deer, W. A., R. A. Howie, and J. Zussman, 1966, An introduction to the rock-forming minerals: London, Longman Group Limited, 528 p.

Dubois, D. P., P. J. Wynne, T. M. Smagala, J. L. Johnson, K. D. Engler, and B. C. McBride, 2004, Geology of Jonah field, Sublette County, Wyoming, *in* J. W. Robinson and K. W. Stanley, eds., Jonah field: Case study of a tight-gas fluvial reservoir: AAPG Studies in Geology 52, p. 37–59.

Hochella Jr., M. F., S. K. Lower, P. A. Maurice, R. L. Penn, N. Sahai, D. L. Sparks, and B. S. Twining, 2008, Nanominerals, mineral nanoparticles, and earth systems: Science, v. 319, p. 1631–1635.

Hunt, J. M., 1996, Petroleum geochemistry and geology: New York, W.H. Freeman and Company, 743 p.

Jimenez-Cruz, F., and G. C. Laredo, 2004, Molecular size evaluation of linear and branched paraffins from the gasoline pool by DFT quantum chemical calculations: Fuel, v. 83, p. 2183–2188.

Katsube, T. J., and D. R. Issler, 1993, Pore-size distribution of shales from the Beaufort-Mackenzie Basin, northern Canada: Current research: Part E: Geological Survey of Canada, Paper 93-1E, p. 123–132.

Katsube, T. J., B. S. Mudford, and M. E. Best, 1991, Petrophysical characteristics of shales from the Scotian shelf: Geophysics, v. 56, no. 10, p. 1681–1689.

Katz, A. J., and A. H. Thompson, 1986, Quantitative prediction of permeability in porous rock: Physical Review B, v. 34, no. 11, p. 8179–8181.

Kilmer, N. H., N. R. Morrow, and J. K. Pitman, 1987, Pressure sensitivity of low permeability sandstones: Journal of Petroleum Science and Engineering, v. 1, p. 65–81.

Kolodzie Jr., S., 1980, Analysis of pore throat size and use of the Waxman-Smits equation to determine OOIP in Spindle field, Colorado: 55th Society of Petroleum Engineers Annual Technical Conference, SPE Paper 9382, 4 p.

Lash, G. G., 2006, Top seal development in the shale-dominated Upper Devonian Catskill delta complex, western New York State: Marine and Petroleum Geology, v. 23, p. 317–335.

Lash, G. G., and D. R. Blood, 2006, The Upper Devonian Rhinestreet black shale of western New York state—Evolution of a hydrocarbon system: 78th Meeting, New York State Geological Association, Sunday B1 Field Trip, p. 223–289.

Luffel, D. L., W. E. Howard, and E. R. Hunt, 1991, Travis Peak core permeability and porosity relationships at reservoir stress: Society of Petroleum Engineers Formation Evaluation, v. 6, no. 3, p. 310–318.

Mitchell, J. K., and K. Soga, 2005, Fundamentals of soil behavior: Hoboken, New Jersey, John Wiley and Sons, 577 p.

Morrow, N. H., 1985, Relationship of pore structure to fluid behavior in low permeability gas sands; year three, final report: New Mexico Energy Research and Development Institute, Santa Fe, New Mexico, NMERDI Report No. 2-72-4309, 158 p.

Nelson, P. H., and M. L. Batzle, 2006, Single-phase permeability, *in* J. Fanchi, ed., Petroleum engineering handbook: General engineering: Richardson, Texas, Society of Petroleum Engineers, v. 1, p. 687–726.

Pittman, E. D., 1979, Porosity, diagenesis, and productive capability of sandstone reservoirs, *in* P. A. Scholle and P. R. Schluger, eds., Aspects of diagenesis: SEPM Special Publication 26, p. 159–173.

Randolph, P. L., D. J. Soeder, and P. Chowdiah, 1984, Porosity and permeability of tight sands: 1984 Society of Petroleum Engineers/U.S. Department of Energy/Gas Research Institute Unconventional Gas Recovery Symposium, Pittsburgh, Pennsylvania, SPE Paper 12836, 10 p.

Rushing, J. A., A. Chaouche, and K. E. Newsham, 2004, A mass balance approach for assessing basin-centered gas prospects: Integrating reservoir engineering, geochemistry and petrophysics, *in* J. M. Cubitt, W. A. England, and S. Larter, eds., Understanding petroleum reservoirs: Toward an integrated reservoir engineering and geochemical approach: Geological Society (London) Special Publications 237, p. 370–390.

Soeder, D. J., and P. Chowdiah, 1990, Pore geometry in high- and low-permeability sandstones, Travis Peak Formation, east Texas: Society of Petroleum Engineers Formation Evaluation, v. 5, no. 4, p. 421–430.

Soeder, D. J., and P. L. Randolph, 1987, Porosity, permeability, and pore structure of the tight Mesaverde Sandstone, Piceance Basin, Colorado: Society of Petroleum Engineers Formation Evaluation, v. 2, no. 2, p. 129–136.

Tissot, B. P., and D. H. Welte, 1978, Petroleum formation and occurrence: Berlin, Springer-Verlag, 538 p.

Wardlaw, N. C., and J. P. Cassan, 1979, Oil recovery efficiency and the rock-pore properties of some sandstone reservoirs: Bulletin of Canadian Petroleum Geology, v. 27, no. 2, p. 117–138.